Progress of Theoretical Physics, Vol. 38, No. 1, July 1967

Interaction between Localized Moments in Metals

Michiko INOUE and Tôru MORIYA

Institute for Solid State Physics
University of Tokyo, Azabu, Tokyo

(Received March 11, 1967)

Interaction energy between two localized moments is calculated on the tight-binding or Wolff-Clogston model by using the Hartree-Fock approximation. A simple general expression is obtained for the effective exchange energy between a distant pair of moments which generally decays as R^{-3} with the oscillations given by the stationary radii of the Fermi surface. Interaction between an adjacent pair of moments is shown to be of local character and its sign is primarily governed by the electronic occupation in the impurity states. A general rule for the sign of the coupling between two moments proposed earlier on the basis of the Anderson model is strongly supported. Possible discontinuous occurrence of localized moments in some alloys is also discussed on the same model.

§ 1. Introduction

Friedel's picture of "virtual bound states" has been remarkably successful for a qualitative understanding of the electronic states of alloys.[1] Two different approaches to treating, at a quantitative level, the problem of a localized magnetic state associated with an impurity atom in metals, were developed out of this picture. The first is the extra-orbital scheme proposed by Anderson,[2] and the second is a tight-binding model due to Wolff and Clogston.[3] The former model is especially suitable for the case of an impurity which has the wave function distinct from that of band electrons, such as a transition element impurity substituted in a host noble metal. The latter, on the other hand, is more appropriate to describe the situation in which the impurity and host metals have the similar type of wave functions, for instance the $3d$ impurity atoms in $4d$ metals. Both models have been extensively investigated in various connections, leading to equivalent results in the case of a single impurity. In particular, many of the important results are deduced from the Hartree-Fock solutions of the models which could account for a wide variety of experimental data.[4]

Studies of the interaction between localized states in metals, so far being reported, are confined to the Anderson scheme. Alexander and Anderson worked out the effect of short range coupling due to the direct covalent admixture between the nearby impurity orbitals, and discussed the underlying physics in terms of the superexchange and double exchange mechanisms.[5] One of the present authors (T.M.) extended their theory and derived a simple qualitative rule governing the alignment of two impurity moments on the adjacent sites.[6]

Downloaded from https://academic.oup.com/ptp/article/38/1/41/1900397 by guest on 21 August 2022

That is, the two moments tend to align themselves antiparallel if the associated orbitals are nearly half-filled, but parallel if they are mostly filled. The effect of long range coupling between moments which in this model arises through the *s-d* interaction, both admixture and exchange types, have been examined by several authors.[7),8)] This coupling leads to either parallel or antiparallel spin alignment depending upon the distance between the two moments and upon the details of the shape of the Fermi surface.

In this article we will examine the interaction between localized moments making use of the Wolff-Clogston tight-binding model. Assumptions and approximations we adopt in the present treatment are as follows: (a) We restrict ourselves to the case of a single non-degenerate band whose Wannier function is well localized on each lattice site. The exchange interaction between the electrons are neglected except at the sites of impurity atoms where the intra-atomic Coulomb repulsion between the electrons with up and down spins, in the sense of Anderson, is essential for magnetization of the localized states. The interaction between localized states arises through the usual itinerant motion of band electrons and also through the additional direct covalent admixture between two impurity atoms when they lie on the nearest neighboring sites. These are summarized in the model Hamiltonian given in § 2. As has been discussed earlier,[4)] physical conclusions drawn out of the Hartree-Fock solutions of this model may be expected to hold in the case of degenerate bands, if we interpret the intra-atomic Coulomb energy U in the non-degenerate model as $U+4J$, J being the intra-atomic exchange energy. (b) We use the Green function formalism within the Hartree-Fock approximation which will be treated in § 3. This approximation may be expected to lead to physically reasonable conclusions for our system except at very low temperature where the Kondo anomaly sets in, and in the limit of low electron density.[4)] (c) A distant pair of impurity atoms are treated by using an asymptotic expansion method. We develop our arguments referring explicitly to the numerical calculations made on a tight-binding band of a simple cubic lattice.

The spin polarization of the host metal, the effect of interaction between a pair of localized moments, and the critical boundaries for the appearance of a moment will be discussed in §§ 4, 5, 6 and 7. By comparing the results of the present and previous studies we aim to find the general features of the interaction, obtainable more or less independent of the initial models. A possible application of the present results to the problem of discontinuous magnetization of 3*d* atoms in 4*d* alloys as proposed by Jaccarino et al.[9)] will be briefly discussed in § 7.

§ 2. Model Hamiltonian

The Hamiltonian for our system is written as

$$\mathcal{H}=\mathcal{H}_0+\mathcal{H}_i\,,$$

Downloaded from https://academic.oup.com/ptp/article/38/1/41/1900397 by guest on 21 August 2022

$$\mathcal{H}_0=\sum_{\sigma}\sum_{j,l} b_{jl}a_{j\sigma}^{*}a_{l\sigma}\,,$$

$$\mathcal{H}_i=E_1\sum_{\sigma} a_{1\sigma}^{*}a_{1\sigma}+U_1a_{1\uparrow}^{*}a_{1\uparrow}a_{1\downarrow}^{*}a_{1\downarrow}+E_2\sum_{\sigma} a_{2\sigma}^{*}a_{2\sigma}+U_2a_{2\uparrow}^{*}a_{2\uparrow}a_{2\downarrow}^{*}a_{2\downarrow}$$
$$+\sum_{\sigma} T_{12}(a_{1\sigma}^{*}a_{2\sigma}+a_{2\sigma}^{*}a_{1\sigma})\,. \qquad (2\cdot1)$$

The first term $\mathcal{H}_0$ is the Hamiltonian for the unperturbed host metal in which $a_{j\sigma}^{*}$ and $a_{j\sigma}$ are the creation and annihilation operators for an electron with spin σ on the j-th site, and b_{jl} is the transfer integral between the Wannier orbitals on the j-th and l-th sites. The term $\mathcal{H}_i$ is the perturbation due to the two impurities denoted by 1 and 2, where E_j stands for the impurity potential, U_j for the intra-atomic Coulomb integral, and T_{12} is the additional transfer integral between the neighboring impurity orbitals; the total transfer integral between the neighboring impurity orbitals are given by $b_{12}+T_{12}$. The eigenvalue of $\mathcal{H}_0$ with the wavevector $\boldsymbol{k}$ follows from the Fourier transform of the transfer integral as

$$\varepsilon_k=\sum_{j} b_{jl}\exp[i\boldsymbol{k}\cdot(\boldsymbol{R}_j-\boldsymbol{R}_l)]\,. \qquad (2\cdot2)$$

In the tight-binding limit for a simple cubic lattice, this becomes

$$\varepsilon_k=-2b(\cos k_xa+\cos k_ya+\cos k_za)\,, \qquad (2\cdot3)$$

where we set the transfer integral negative, i.e. $b>0$, so that the bottom of the band lies at point $\boldsymbol{k}=0$.

§ 3. Hartree-Fock solutions

We start with the resolvent form of the one-particle Green's function given by

$$G(\epsilon+is)=(\epsilon+is-\mathcal{H})^{-1}$$
$$=(\epsilon+is-\mathcal{H}_0)^{-1}+(\epsilon+is-\mathcal{H}_0)^{-1}\mathcal{H}_i(\epsilon+is-\mathcal{H})^{-1},$$
$$(s\to+0),$$

where we take for $\mathcal{H}$ the Hartree-Fock Hamiltonian derived from (2·1). In the localized state representation, we have

$$G_{jl}^{\sigma}=g_{jl}+(g_{j1}V_1^{\sigma}+g_{j2}T_{12})G_{1l}^{\sigma}+(g_{j2}V_2^{\sigma}+g_{j1}T_{12})G_{2l}^{\sigma}\,. \qquad (3\cdot1)$$

Here g_{jl} is the Green function for the unperturbed band:

$$g_{jl}(\epsilon+is)=N^{-1}\sum_{k}(\epsilon+is-\epsilon_k)^{-1}\exp[i\boldsymbol{k}\cdot(\boldsymbol{R}_j-\boldsymbol{R}_l)]\,, \qquad (3\cdot2)$$

and V_i^{σ} is the Hartree-Fock potential of the i-th impurity,

$$V_i^{\sigma}=E_i+U_iN_i^{-\sigma},$$

N_i^{σ} being the number of localized electrons with spin σ of the i-th atom. The

Downloaded from https://academic.oup.com/ptp/article/38/1/41/1900397 by guest on 21 August 2022

diagonal element of the Green function is obtained from (3·1) as

$$G_{jj}^{\sigma}=g_{jj}+\{V_1^{\sigma}g_{j1}g_{1j}+V_2^{\sigma}g_{j2}g_{2j}+T_{12}(g_{j2}g_{1j}+g_{j1}g_{2j})$$
$$+(V_1^{\sigma}V_2^{\sigma}-T_{12}^2)[g_{j1}(g_{12}g_{2j}-g_{11}g_{1j})+g_{j2}(g_{21}g_{1j}-g_{22}g_{2j})]\}$$
$$\times\{1-(V_1^{\sigma}+V_2^{\sigma})g_{11}-T_{12}(g_{12}+g_{21})+(V_1^{\sigma}V_2^{\sigma}-T_{12}^2)(g_{11}^2-g_{12}g_{21})\}^{-1}. \tag{3·3}$$

The number of the electrons with spin σ of the j-th atom is evaluated from

$$n_j^{\sigma}=\int^{\epsilon_F}d\epsilon\,\rho_j^{\sigma}(\epsilon)=-\pi^{-1}\,\mathrm{Im}\int^{\epsilon_F}d\epsilon G_{jj}^{\sigma}(\epsilon). \tag{3·4}$$

Equation (3·4) together with Eq. (3·3) gives the self-consistency condition for $N_j^{\uparrow}$ and $N_j^{\downarrow}$ of the j-th impurity atom.

§ 4. Spin polarization around an impurity atom

We shall discuss in this section the spatial distribution of the spin polarization around an impurity atom. For this purpose we put $V_2^{\sigma}=0$, $T_{12}=0$ in the relevant expressions derived in the previous section and introduce a notation with a bar to refer to the quantities in the presence of a single impurity atom. From Eqs. (3·3) and (3·4) the deviation in the number of localized electrons with spin σ of the j-th atom from its unperturbed value is given by

$$\delta\bar{n}_{j(1)}^{\sigma}=-\pi^{-1}\,\mathrm{Im}\int^{\epsilon_F}d\epsilon[\bar{G}_{jj}^{\sigma}(\epsilon)-g_{jj}(\epsilon)]$$
$$=-\pi^{-1}\,\mathrm{Im}\int^{\epsilon_F}d\epsilon\,\bar{V}_1^{\sigma}g_{j1}(\varepsilon)g_{1j}(\varepsilon)[1-\bar{V}_1^{\sigma}g_{jj}(\epsilon)]^{-1}. \tag{4·1}$$

The change in number of electrons and the spin polarization of the same atom are defined by

$$\left.\begin{matrix}\delta\bar{n}_{j(1)}\\ \bar{m}_{j(1)}\end{matrix}\right\}=\delta\bar{n}_{j(1)}^{\uparrow}\pm\delta\bar{n}_{j(1)}^{\downarrow}. \tag{4·2}$$

By taking a sum of $\delta\bar{n}_{j(1)}^{\sigma}$ over all the lattice sites we get the following expression for the change in total number of electrons with spin σ:

$$\delta\bar{n}_{(1)}^{\sigma}=\sum_j\delta\bar{n}_{j(1)}^{\sigma}=-\pi^{-1}\,\mathrm{Im}\log[1-\bar{V}_1^{\sigma}g_{11}(\epsilon_F)]=\pi^{-1}\gamma_1^{\sigma}(\epsilon_F), \tag{4·3}$$

where $\gamma_1^{\sigma}(\epsilon_F)$ is the phase shift at the Fermi level caused by the impurity potential $\bar{V}_1^{\sigma}$. Finally the host-metal spin polarization is given by

$$\bar{m}_h=\delta\bar{n}_h^{\uparrow}-\delta\bar{n}_h^{\downarrow},\quad\text{with}\quad\delta\bar{n}_h^{\sigma}=\delta\bar{n}_{(1)}^{\sigma}-\delta\bar{N}_1^{\sigma}. \tag{4·4}$$

As has been discussed earlier,[4),10)] the total spin polarization in the host metal is rather insensitive to the details of the band structure, and the sign of

Downloaded from https://academic.oup.com/ptp/article/38/1/41/1900397 by guest on 21 August 2022

the spin polarization is governed mainly by the electron occupation in the host metal band and in the impurity atom; the spin polarization in the host metal is antiparallel to the impurity moment when the band as well as the impurity orbitals are nearly half-filled, while the parallel spin polarization tends to be favored as they get more filled.

Since the main part of the spin polarization should be well localized around an impurity atom, we expect the spin polarization of the nearest neighboring atoms obey the same rule as that stated above for the total spin polarization in the host metal, provided the transfer integral b_{jl} is of short range. This is supported by the numerical calculation for the simple cubic lattice as will be shown below.

The spin polarization in the range far from the impurity atom, to which the electrons near the Fermi surface mainly contribute, decays as R^{-3} with the oscillation whose period is determined by the shape of the Fermi surface. This behavior can be obtained by using an asymptotic expansion for large R. As will be illustrated for the case of a simple cubic lattice, this expansion is expected to be valid approximately in many cases, even at fairly short distance from the impurity atom, say at the second neighbor sites.

In this way we can get a fairly good picture for the spatial distribution of the spin polarization in the entire crystal. If the asymptotic expression for the spin polarization is applied to the range outside the nearest neighbor shell, the spin polarization at the nearest neighbors is obtained by subtracting from the total spin polarization (4·4) the sum of this asymptotic expressions over all the lattice points outside the nearest neighbor shell.

(a) *asymptotic expression for large R*

In order to get an asymptotic expression for large R of Eq. (4·1), we first calculate the asymptotic expression for the unperturbed Green function given by Eq. (3·2) and rewritten here as

$$g_R(\epsilon)=N^{-1}\sum_k(\epsilon+is-\epsilon_k)^{-1}\exp(i\boldsymbol{k}\cdot\boldsymbol{R})=F_R(\epsilon)-i\pi\eta_R(\epsilon). \tag{4·5}$$

The imaginary part of the above expression $\eta_R(\epsilon)$ is reduced to a surface integral in the $\boldsymbol{k}$-space as follows:

$$\begin{aligned}\eta_R(\epsilon)&=v_0(2\pi)^{-3}\iint_{\epsilon_k=\epsilon}dS|\nabla\epsilon_k|^{-1}\exp(i\boldsymbol{k}\cdot\boldsymbol{R})\\&=v_0(2\pi)^{-3}\iint_{\epsilon_k=\epsilon}dk_xdk_y|\partial\epsilon/\partial k_z|^{-1}\cos(k_zR),\end{aligned} \tag{4·6}$$

where v_0 is the atomic volume and the z axis is assumed to be parallel to $\boldsymbol{R}$. The real part $F_R(\epsilon)$ is given by a Hilbert transform of $\eta_R(\epsilon)$, i.e.

$$F_R(\epsilon)=\mathcal{P}\int_{-\infty}^{\infty}d\epsilon'(\epsilon-\epsilon')^{-1}\eta_R(\epsilon'). \tag{4·7}$$

Downloaded from https://academic.oup.com/ptp/article/38/1/41/1900397 by guest on 21 August 2022

The dominant term in the asymptotic expansion of (4·6) is obtained by using the stationary phase method;[11] the main contribution to the integral in (4·6) comes from the stationary points $\boldsymbol{k}_j$ on the energy surface $\epsilon=\epsilon_k$, where $\nabla\epsilon_k$ is parallel to $\boldsymbol{R}$. When the effective mass components at the stationary points $\boldsymbol{k}_j$ are finite, as is usually the case, we get after some calculation

$$g_R(\epsilon) = -(v_0/2\pi)R^{-1}\sum_j' |m_2^*(\boldsymbol{k}_j)m_3^*(\boldsymbol{k}_j)|^{1/2}\exp[i(\boldsymbol{k}_j\cdot\boldsymbol{R}+\varphi_j)] \qquad (4\cdot8)$$

with

$$\varphi_j=\begin{cases}0 & \text{for } m_2^*(\boldsymbol{k}_j)>0\,,\ m_3^*(\boldsymbol{k}_j)>0\,,\\ \pi/2 & \text{for } m_2^*(\boldsymbol{k}_j)m_3^*(\boldsymbol{k}_j)<0\,,\\ \pi & \text{for } m_2^*(\boldsymbol{k}_j)<0\,,\ m_3^*(\boldsymbol{k}_j)<0\,,\end{cases}$$

where $m_2^*(\boldsymbol{k}_j)$ and $m_3^*(\boldsymbol{k}_j)$ are the principal values of the effective mass tensor in the directions perpendicular to $\boldsymbol{R}$, and $\boldsymbol{k}_j$ is the stationary point on the energy surface where the following condition is satisfied:

$$\nabla\epsilon_k=\boldsymbol{R}|\nabla\epsilon_k|/|\boldsymbol{R}|. \qquad (4\cdot9)$$

One can find at least one stationary point on the energy surface except when the energy surface passes through the Van Hove critical point, which is specified by $\nabla\epsilon_k=0$. In the latter case one cannot always find a stationary point depending on the direction of $\boldsymbol{R}$.*)

Inserting the asymptotic expression (4·8) for $g_R(\epsilon)$ into Eq. (4·1), one obtains after a partial integration

$$\begin{aligned}\delta\bar{n}^\sigma(\boldsymbol{R}) = {}& (v_0^2/4\pi R^3)\,\mathrm{Re}\,\bar{V}_1{}^\sigma[1-\bar{V}_1{}^\sigma g_{11}(\epsilon_F)]^{-1}\sum_{j,j'}'\{|\nabla\epsilon(\boldsymbol{k}_j)|^{-1}+|\nabla\epsilon(\boldsymbol{k}_{j'})|^{-1}\}^{-1}\\ &\times|m_2^*(\boldsymbol{k}_j)m_3^*(\boldsymbol{k}_j)m_2^*(\boldsymbol{k}_{j'})m_3^*(\boldsymbol{k}_{j'})|^{1/2}\exp i[(\boldsymbol{k}_j+\boldsymbol{k}_{j'})\cdot\boldsymbol{R}+\varphi_j+\varphi_{j'}]\\ &+0(R^{-4}). \qquad (4\cdot10\mathrm{a})\end{aligned}$$

This expression is rewritten in terms of the phase shifts as

$$\begin{aligned}\delta\bar{n}^\sigma(\boldsymbol{R}) = {}& (v_0^2/4\pi R^3)[\pi\eta(\epsilon_F)]^{-1}\sum_{j,j'}'\{|\nabla\epsilon(\boldsymbol{k}_j)|^{-1}+|\nabla\epsilon(\boldsymbol{k}_{j'})|^{-1}\}^{-1}\\ &\times|m_2^*(\boldsymbol{k}_j)m_3^*(\boldsymbol{k}_j)m_2^*(\boldsymbol{k}_{j'})m_3^*(\boldsymbol{k}_{j'})|^{1/2}\sin\gamma^\sigma(\epsilon_F)\\ &\times\cos[(\boldsymbol{k}_j+\boldsymbol{k}_{j'})\cdot\boldsymbol{R}+\gamma^\sigma(\epsilon_F)+\varphi_j+\varphi_{j'}] \qquad (4\cdot10\mathrm{b})\end{aligned}$$

where $\eta(\epsilon_F)$ is the density of states at the Fermi level of the unperturbed band,

*) When there is no stationary point the above treatment using the stationary phase method fails. Moreover, the asymptotic expansion generally fails when the energy surface passes through the Van Hove critical point $\boldsymbol{k}_c$, since we have a term in $g_R(\epsilon)$, which is proportional to $R^{-1}\exp[-|\epsilon-\epsilon(\boldsymbol{k}_c)|^{1/2}R]$ near this point and cannot be included in the asymptotic expansion.

Downloaded from https://academic.oup.com/ptp/article/38/1/41/1900397 by guest on 21 August 2022

and $\boldsymbol{k}_j$ and $\boldsymbol{k}_{j'}$ represent the stationary points on the Fermi surface. Equation (4·10b) illustrates the familiar feature that the screening charge density decays as R^{-3} with the oscillation whose period is determined by the shape of the Fermi surface.[1),12)] When one or two of the effective mass components diverges on the Fermi surface, the stationary section of the Fermi surface is no longer a point but a line or a plane. In these cases we have R^{-2} and R^{-1} decays of $\delta\bar{n}(R)$, respectively. The first case is encountered in the simple cubic lattice for $\boldsymbol{R}$ along the $\langle 110\rangle$ axis and the Fermi level at two-thirds of the band width. The second case is realized in the body-centered cubic lattice for $\boldsymbol{R}$ along $\langle 100\rangle$ axis when the band is half-filled.

(b) *numerical results for a simple cubic lattice*

The results of the direct numerical estimation of the quantities given by Eqs. (4·1)–(4·4) for a simple cubic lattice are summarized in the first four

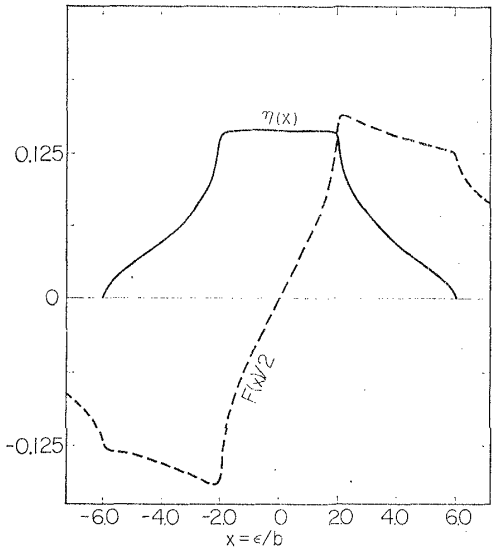

Fig. 1. Density of states (full curve) and its Hilbert transform (dashed curve) for a simple cubic band.

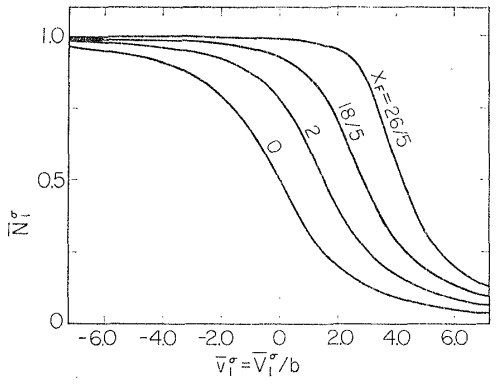

Fig. 2. Number of electrons with spin σ in an impurity atom versus the impurity potential, for different values of the Fermi level.

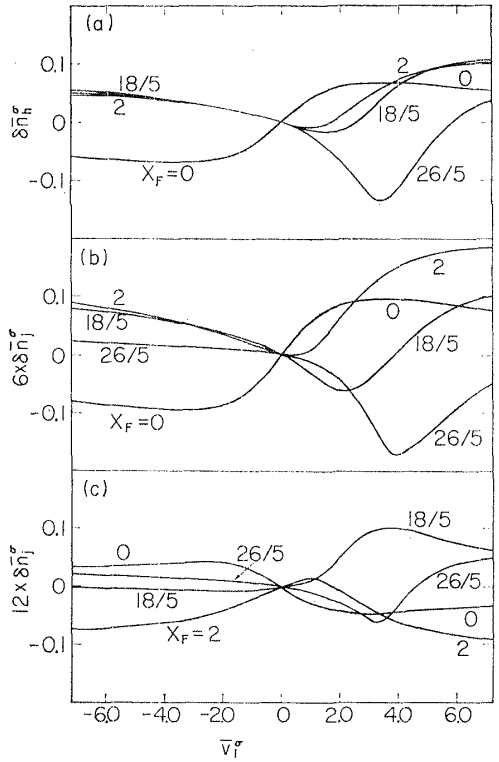

Fig. 3. Changes in number of electrons with spin σ on the surrounding sites of an impurity are plotted as a function of the impurity potential varying the Fermi level: (a) the host metal, (b) the first neighboring atoms and (c) the second neighboring atoms.

Downloaded from https://academic.oup.com/ptp/article/38/1/41/1900397 by guest on 21 August 2022

figures.*) Figure 1 shows the unperturbed density of states $\eta(\epsilon)$ and its Hilbert transform $F(\epsilon)$. In Figs. 2 and 3 we draw the curves for $\overline{N}_1^{\sigma}$, $\delta\overline{n}_h^{\sigma}$ and $\delta\overline{n}_j^{\sigma}$ up to the second neighboring sites, as a function of $\overline{V}_1^{\sigma}$ varying the Fermi level

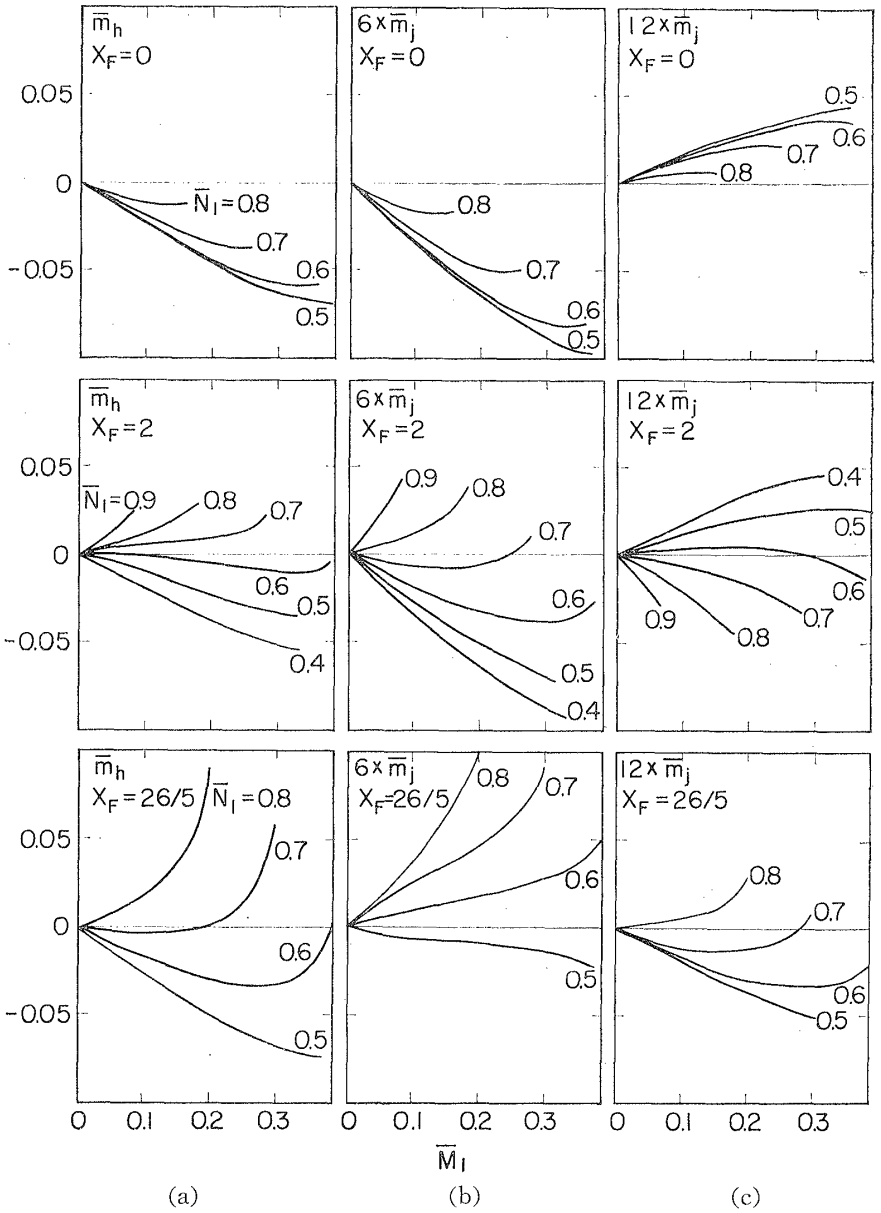

Fig. 4. Induced moments around an impurity atom versus the impurity moment: (a) the host metal, (b) the first impurity atoms and (c) the second neighboring atoms.

*) The numerical calculations have been carried out on FACOM 202 of ISSP. We have employed the method of Koster and Slater[13] to evaluate $g_{jl}(\epsilon)$. The numerical accuracy is considered to be sufficient for the present purpose from the fact that the normalization error for $\eta(\epsilon)$ is less than 1 percent. However, the accuracy seems to be insufficient to reproduce the sharp cusps in the density of states curve at the Van Hove singular points (see Fig. 1).

Downloaded from https://academic.oup.com/ptp/article/38/1/41/1900397 by guest on 21 August 2022

as a parameter. In Fig. 4 we replot from Fig. 3 the induced spin polarization $\bar{m}_h$ and $\bar{m}_j$ against $\bar{M}_1$, the impurity moment.

Some interesting features emerge out of these figures. In the first place, remarkable similarity between Figs. 4a and 4b indicates that the behavior of the induced moment at the nearest neighboring sites of an impurity is similar to that of the total spin polarization of the host metal. This is especially so when the impurity atom has a large moment. Therefore the rule for the sign of the total spin polarization as stated above holds equally for the nearest neighbor atoms. Secondly, the relative sign of the spin polarization at the second neighbor site depends on the position of the Fermi level, although there is a definite tendency that the induced polarization changes sign as one goes from the nearest to the second neighbor sites. This change of sign is considered to come from the oscillation of the screening charge density as was discussed in (a). In order to get some feeling as to how adequate the asymptotic formula is to represent the exact behavior of $\delta\bar{n}^{\sigma}(\boldsymbol{R})$, Eq. (4·10b) is evaluated for the simple cubic lattice. In Fig. 5 we plot $\bar{m}_j$ on the second neighbor site against $\bar{M}_1$. It should be noted here that these curves reproduce fairly well the characteristic features of the exact results given in Fig. 3c. From these results we may expect that in the presence of a large impurity moment it is reasonably safe to discuss qualitatively the spatial distribution of the host metal polarization beyond the nearest neighboring sites on the basis of asymptotic formula. This simplifies a great deal what would otherwise need a tedious computations.

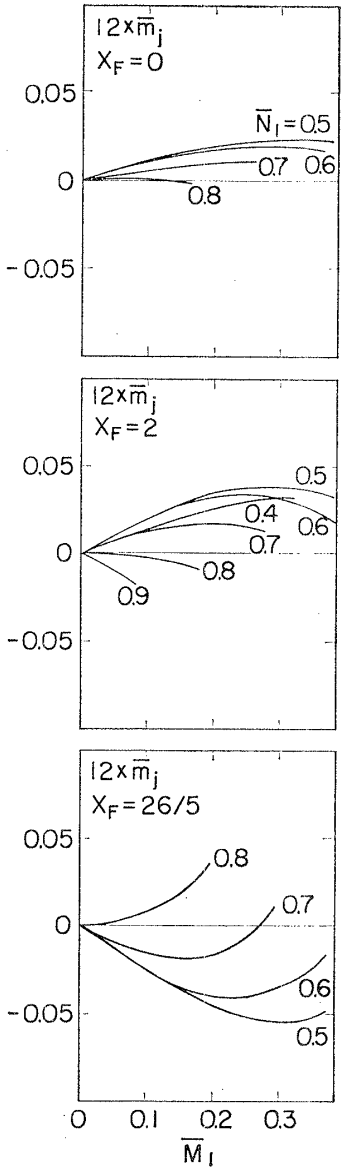

Fig. 5. Induced moments at the second neighboring sites of an impurity atom versus the impurity moment, calculated by the asymptotic formula (4·10).

§ 5. Interaction between localized moments

Let us now investigate the interaction between the two localized moments. A change in the Hartree-Fock energy due to the presence of two impurity moments is evaluated by

$$\delta E(1,2)=\sum_{\sigma}\sum_{j}\int^{\epsilon_F} d\epsilon\,(\epsilon-\epsilon_F)\,\delta\rho_j{}^{\sigma}-U_1N_1^{\uparrow}N_1^{\downarrow}-U_2N_2^{\uparrow}N_2^{\downarrow}, \qquad (5\cdot1)$$

Downloaded from https://academic.oup.com/ptp/article/38/1/41/1900397 by guest on 21 August 2022

where

$$\delta\rho_j{}^\sigma = -\pi^{-1}\,\mathrm{Im}[G_{jj}^\sigma(\epsilon) - g_{jj}(\epsilon)].$$

Similarly a change in the Hartree-Fock energy for the system with a single impurity is given by

$$\delta\bar{E}(1) = \sum_\sigma \sum_j \int^{\epsilon_F} d\epsilon\,(\epsilon - \epsilon_F)\,\delta\bar{\rho}_j{}^\sigma - U_1\bar{N}_1^\uparrow\bar{N}_1^\downarrow. \tag{5·2}$$

The interaction energy of the two moments is defined by

$$E = \delta E(1,2) - \delta\bar{E}(1) - \delta\bar{E}(2). \tag{5·3}$$

From Eqs. (5·1), (5·2) and (5·3) one gets after a partial integration

$$\begin{aligned} E = -\int^{\epsilon_F} d\epsilon\,[\delta n_{(1,2)}^\sigma - \delta\bar{n}_{(1)}^\sigma - \delta\bar{n}_{(2)}^\sigma] - U_1(N_1^\uparrow N_1^\downarrow - \bar{N}_1^\uparrow\bar{N}_1^\downarrow) \\ - U_2(N_2^\uparrow N_2^\downarrow - \bar{N}_2^\uparrow\bar{N}_2^\downarrow), \end{aligned} \tag{5·4}$$

where $\delta\bar{n}_{(1)}^\sigma$ is given by Eq. (4·3) with $\epsilon_F = \epsilon$ and similarly $\delta n_{(1,2)}^\sigma$ is obtained by summing Eq. (3·3) for $G_{jj}^\sigma(\epsilon)$ over all sites. We have

$$\begin{aligned} \delta n_{(1,2)}^\sigma = -\pi^{-1}\,\mathrm{Im}\log\,[1 - (V_1{}^\sigma - V_2{}^\sigma)g_{11}(\epsilon) - T_{12}[g_{12}(\epsilon) + g_{21}(\epsilon)] \\ + (V_1{}^\sigma V_2{}^\sigma - T_{12}^2)\,\{[g_{11}(\epsilon)]^2 - g_{12}(\epsilon)g_{21}(\epsilon)\}]. \end{aligned} \tag{5·5}$$

Here we shall not undertake an elaborate procedure of solving Eq. (5·5) self-consistently. Instead, we consider specifically the case in which the coupling energy is sufficiently small compared with the intra-atomic Coulomb energy U, so that the effect of interaction with another lacalized moment may be treated as a perturbation to the individual moment which is stably polarized on account of its own U. We denote the change in number of electrons with spin σ on an individual impurity atom due to the coupling with the other impurity by

$$N_j{}^\sigma = \bar{N}_j{}^\sigma + \Delta N_j{}^\sigma, \qquad j = 1, 2. \tag{5·6}$$

Then for small deviations, we may develop Eq. (5·5) in power series of $\Delta N_j{}^\sigma$, and derive, in the lowest order in ΔN_j, the following expression for the interaction energy:

$$\begin{aligned} E = \sum_\sigma \{ & \bar{V}_1{}^\sigma \bar{V}_2{}^\sigma (\bar{V}_1{}^\sigma - \bar{V}_2{}^\sigma)^{-1}[\delta\bar{n}_{2(1)}^\sigma - \delta\bar{n}_{1(2)}^\sigma] \\ & - 2T_{12}(\bar{V}_1{}^\sigma - \bar{V}_2{}^\sigma)^{-1}[\bar{V}_1{}^\sigma \bar{f}_{2(1)}^\sigma - \bar{V}_2{}^\sigma \bar{f}_{1(2)}^\sigma] \\ & + T_{12}^2(\bar{V}_1{}^\sigma - \bar{V}_2{}^\sigma)^{-1}(\bar{N}_1{}^\sigma - \bar{N}_2{}^\sigma)\} \\ \equiv & E^{(1)} + E^{(2)} + E^{(3)} \end{aligned} \tag{5·7}$$

with

$$\bar{f}_{2(1)}^\sigma = \pi^{-1}\,\mathrm{Im}\int^{\epsilon_F} d\epsilon\,[1 - \bar{V}_1{}^\sigma g_{11}(\epsilon)]^{-1} g_{12}(\epsilon), \text{ etc.} \tag{5·8}$$

Downloaded from https://academic.oup.com/ptp/article/38/1/41/1900397 by guest on 21 August 2022

For later convenience, let us rewrite Eq. (5·7) in terms of parameters normalized to the transfer integral $-b$ between the nearest neighboring atoms in the host metal. We have

$$E^{(1)}/b=\sum_{\sigma}\bar{v}_1{}^{\sigma}\bar{v}_2{}^{\sigma}(\bar{v}_1{}^{\sigma}-\bar{v}_2{}^{\sigma})^{-1}[\delta\bar{n}^{\sigma}_{2(1)}-\delta\bar{n}^{\sigma}_{1(2)}]\,,$$

$$E^{(2)}/b=2t\sum_{\sigma}(\bar{v}_1{}^{\sigma}-\bar{v}_2{}^{\sigma})^{-1}[\bar{v}_1{}^{\sigma}\bar{f}^{\sigma}_{2(1)}-\bar{v}_2{}^{\sigma}\bar{f}^{\sigma}_{1(2)}]\,,$$

$$E^{(3)}/b=t^2\sum_{\sigma}(\bar{v}_1{}^{\sigma}-\bar{v}_2{}^{\sigma})^{-1}(\bar{N}_1{}^{\sigma}-\bar{N}_2{}^{\sigma}), \tag{5·7a}$$

where

$$\bar{v}_1{}^{\sigma}=\bar{V}_1{}^{\sigma}/b\,,\qquad t=T/(-b). \tag{5·9}$$

The exchange energy may be defined by half the difference in the interaction energy between a pair of parallel and antiparallel moments, suth that

$$E_{ex}=(E_{\uparrow\uparrow}-E_{\uparrow\downarrow})/2\,. \tag{5·10}$$

When the two impurity atoms are not neighboring with each other, the additional transfer integral T_{12} between them may be neglected; and it is sufficient to take only the first term in Eq. (5·7). When one treat a pair of impurity atoms near to each other, all the three terms in (5·7) should be taken into account. In what follows we shall discuss the cases of a distant pair and an adjacent pair separately.

(i) *coupling between a distant pair*

We can neglect the terms containing T_{12} in Eq. (5·7) and replace $\delta\bar{n}^{\sigma}_{1(2)}$ by its asymptotic expression given by Eq. (4·10). Thus the exchange energy (5·10) is reduced to

$$\begin{aligned}E_{ex}=E^{(1)}_{ex}=(v_0{}^2/8\pi^3R^3)\,[\pi\eta(\epsilon_F)]^{-2}\sum_{j,j'}\{|\nabla\epsilon(\boldsymbol{k}_j)|^{-1}+|\nabla\epsilon(\boldsymbol{k}_{j'})|^{-1}\}^{-1}\\ \times|m_2{}^*(\boldsymbol{k}_j)m_3{}^*(\boldsymbol{k}_j)m_2{}^*(\boldsymbol{k}_{j'})m_3{}^*(\boldsymbol{k}_{j'})|^{1/2}\sin\pi\bar{m}_{(1)}\sin\pi\bar{m}_{(2)}\\ \times\cos[(\boldsymbol{k}_j+\boldsymbol{k}_{j'})\cdot\boldsymbol{R}+\pi\delta\bar{n}_{(1)}+\pi\delta\bar{n}_{(2)}+\varphi_j+\varphi_{j'}],\end{aligned} \tag{5·11}$$

where

$$\left.\begin{matrix}\delta\bar{n}_{(i)}\\ \bar{m}_{(i)}\end{matrix}\right\}=\delta\bar{n}^{\uparrow}_{(i)}\pm\delta\bar{n}^{\downarrow}_{(i)}=\pi^{-1}[\gamma_i{}^{\uparrow}(\epsilon_F)\pm\gamma_i{}^{\downarrow}(\epsilon_F)]\,,$$

and $\boldsymbol{k}_j$ denotes the stationary point on the Fermi surface. It is noteworthy that the above formula for E_{ex} contains no ambiguous extra parameter, but is expressed in terms of the quantities associated with the Fermi surface and the overall polarization and deviation in the number of electrons due to the impurity atom. The sign of the interaction between the two moments oscillates with a period determined by the stationary radii of the Fermi surface. It is also of interest

Downloaded from https://academic.oup.com/ptp/article/38/1/41/1900397 by guest on 21 August 2022

to note that if we take the free electron spectrum for $\epsilon(\boldsymbol{k})$, the above expression reduces to the one obtained by Caroli on the Anderson model.[8)]

(ii) *coupling between neighboring atoms*

We now turn to the interaction between an adjacent pair of localized moments. In this case the full expression of Eq. (5·7) should be used, since the transfer integral between the neighboring impurities is generally different from that in the original band, i.e. T_{12} is not negligible.

The first term on the right-hand side of (5·7) is rewritten as

$$E^{(1)} = -\sum_{\sigma} \{\pi\eta(\epsilon_F) \sin \pi(\delta\bar{n}^{\sigma}_{(1)} - \delta\bar{n}^{\sigma}_{(2)})\}^{-1} \sin \pi\delta\bar{n}^{\sigma}_{(1)} \sin \pi\delta\bar{n}^{\sigma}_{(2)} \times [\delta\bar{n}^{\sigma}_{2(1)} - \delta\bar{n}^{\sigma}_{1(2)}], \tag{5·12}$$

where $\delta\bar{n}^{\sigma}_{(i)}$ can be estimated from the valency and the moment of the i-th impurity atom, while $\delta\bar{n}^{\sigma}_{2(1)}$, etc., have been given in the preceding section. As was discussed in the preceding section, the spin polarization and the change in the electronic occupation of the nearest neighboring atoms are quite similar to the corresponding quantities for the entire host metal, which is rather insensitive to the details of the band structure. This situation is in contrast to the case of long range coupling. Therefore, we may expect that the results obtained for the simple cubic lattice have fairly general validity. Figure 6 shows the numerical

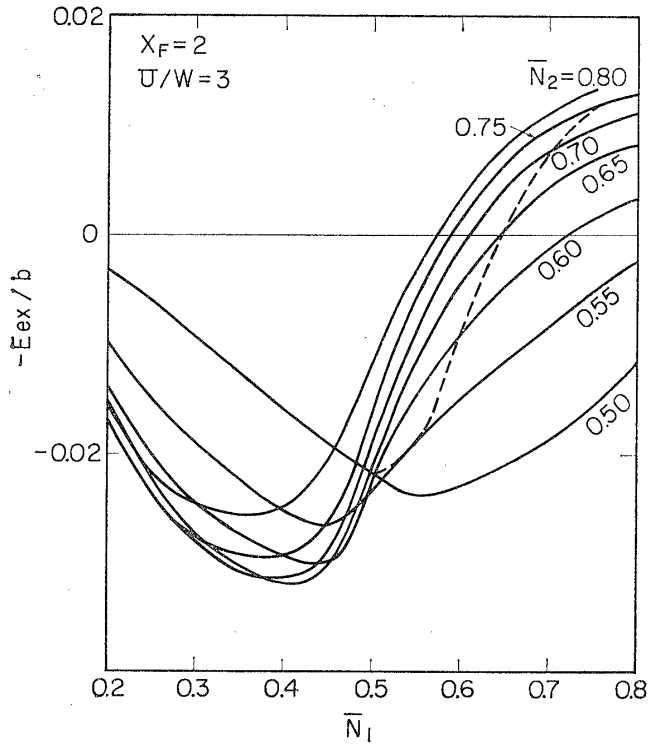

Fig. 6. The exchange energy $E_{ex}^{(1)}$, between two neighboring impurities with the numbers of electrons $\bar{N}_1$ and $\bar{N}_2$, calculated with the first equation of (5·7a) for $x_F=2$ and $U/w=3$ on energy scale given by (5·9) and (5·13).

Downloaded from https://academic.oup.com/ptp/article/38/1/41/1900397 by guest on 21 August 2022

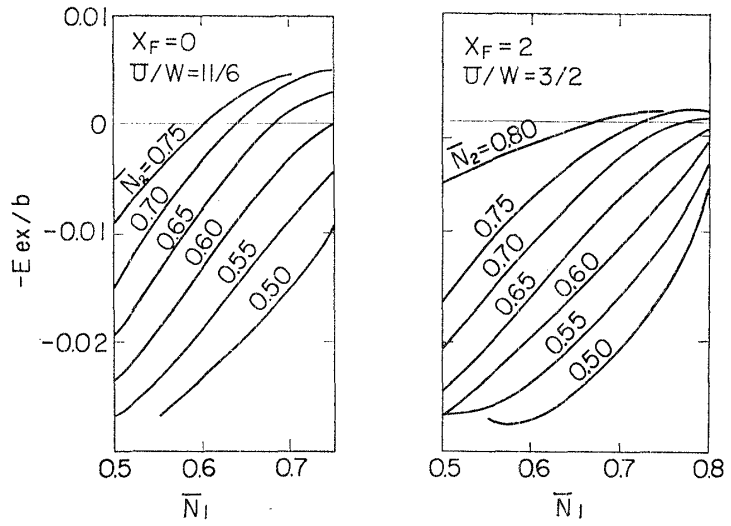

Fig. 7. The exchange energy $E_{ex}^{(1)}$ for different values of parameters: (a) $x_F=0$, $U/w=11/6$, and (b) $x_F=2$, $U/w=3/2$.

results for the simple cubic lattice of $E_{ex}^{(1)}=(E_{\uparrow\uparrow}^{(1)}-E_{\uparrow\downarrow}^{(1)})/2$ as a function of $\bar{N}_1$ and $\bar{N}_2$ for a fixed value of $U=U_1=U_2$. It is noticeable that the curves in Fig. 6 bear a strong resemblance to those obtained earlier on the basis of Anderson model.[6] Therefore, we may expect the same general rule as that mentioned earlier[4),6)] to hold for the sign of the interaction between an adjacent pair of localized moments; this rule is determined mainly by the occupation number of electrons in the two atoms. There is in fact some evidence in favor of this statement: the curve for $E_{ex}^{(1)}$ is less sensitive to the position of the Fermi level, and the decreasing U is to increase the tendency to antiparallel spin alignment as is seen from Fig. 7.

The last term $E^{(3)}$ in (5·7) is easy to interpret, since this expression takes exactly the same form as that derived on the basis of the Anderson model.[6] The function $E_{ex}^{(3)}$ for the simple cubic lattice is plotted in Fig. 8. One easily notices the similarity between Figs. 6 and 8, as is naturally expected from the above argument.

It remains to discuss the effect of the interference term $E^{(2)}$. Since this is the interference effect between $E^{(1)}$ and $E^{(3)}$ which are shown to behave similarly as functions of $\bar{V}_i^{\sigma}$ or $\bar{N}_i^{\sigma}$, we may expect that this term also shows behavior similar to them except for the sign.

When the transfer integral is of short range and vanishes except for the nearest neighboring pairs, we have

$$g_{12}(\epsilon)=z^{-1}[1-\epsilon g_{11}(\epsilon)],$$

where z is the number of nearest neighbors. Equation (5·8) now reduces to

$$\bar{f}_{2(1)}^{\sigma}=z^{-1}\int^{x_F}dx(x-\bar{v}_1^{\sigma})\eta(x)\{[1-\bar{v}_1^{\sigma}F(x)]^2+[\pi\bar{v}_1^{\sigma}\eta(x)]^2\}^{-1} \quad (5\cdot13)$$

Downloaded from https://academic.oup.com/ptp/article/38/1/41/1900397 by guest on 21 August 2022

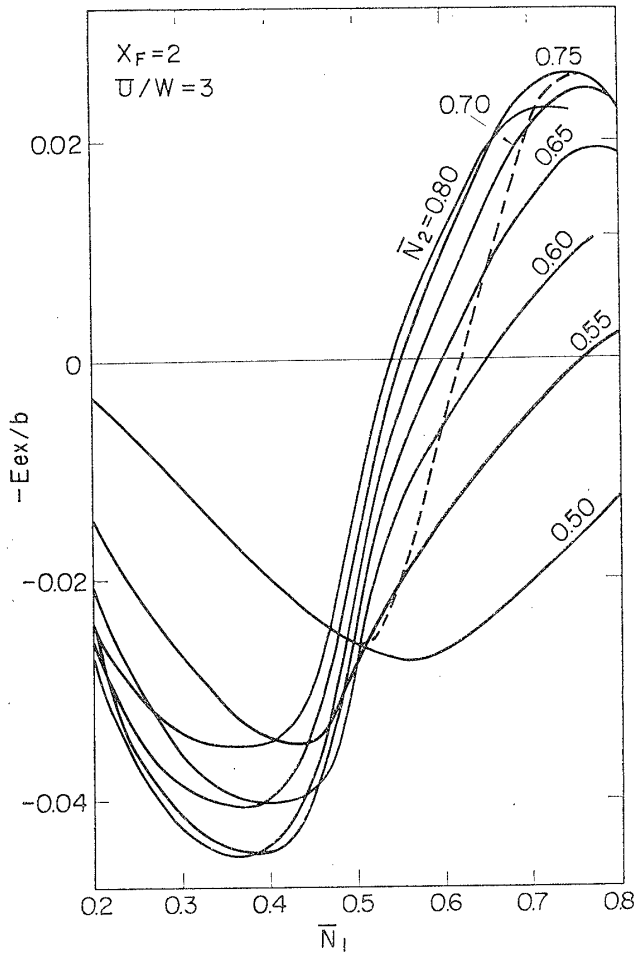

Fig. 8. The exchange energy $E_{ex}^{(3)}$ calculated with the third equation of (5·7a) for $x_F=2$ and $U/w=3$.

with

$$x=\epsilon/b\,,\qquad x_F=\epsilon_F/b\,,\qquad b^{-1}g_{11}(\epsilon)=F(x)-i\pi\eta(x)\,. \tag{5·13}$$

Asymptotic behavior for large $|\bar{v}_1{}^\sigma|$ of $\bar{f}^\sigma_{2(1)}$ is described as follows:

$$\bar{v}_1{}^\sigma \bar{f}^\sigma_{2(1)}\sim\begin{cases}1-A(x_F)-[B(x_F)/\bar{v}_1{}^\sigma]+0(1/\bar{v}_1{}^\sigma)^2 & \text{for}\quad \bar{v}_1\to-\infty\,,\\ -A(x_F)+[B(x_F)/\bar{v}_1{}^\sigma]+0(1/\bar{v}_1{}^\sigma)^2 & \text{for}\quad \bar{v}_1\to+\infty\end{cases} \tag{5·14}$$

with

$$A(x_F)=z^{-1}\int_{-z}^{x_F}dx\,\eta(x)\,\{[F(x)]^2+[\pi\eta(x)]^2\}^{-1},$$

$$B(x_F)=z^{-1}\int_{-z}^{x_F}dx\,\eta(x)\,\{[F(x)]^2+[\pi\eta(x)]^2\}^{-1}[x-2F(x)\,\{[F(x)]^2+[\pi\eta(x)]^2\}^{-1}]\,. \tag{5·15}$$

Downloaded from https://academic.oup.com/ptp/article/38/1/41/1900397 by guest on 21 August 2022

Thus $\bar{v}_1{}^\sigma \bar{f}^\sigma_{2(1)}$ varies from $1-A$ to $-A$ as $\bar{v}_1{}^\sigma$ varies from $-\infty$ to $+\infty$. It is also easy to see that a bound state is formed outside the original band when $\bar{v}_1{}^\sigma \gtrless (z-1)$ is satisfied. This means that the variation of $\bar{v}_1{}^\sigma \bar{f}^\sigma_{2(1)}$ from $1-A$ to $-A$ as a function of $\bar{v}_1{}^\sigma$ takes place mainly in the range $-z<\bar{v}_1{}^\sigma<z$. Since we have $\bar{v}_1{}^\sigma \bar{f}^\sigma_{2(1)}=0$ for $\bar{v}_1{}^\sigma=0$, we may further expect that the main part of variation of $\bar{v}_1{}^\sigma \bar{f}^\sigma_{2(1)}$ takes place in the upper part of the above range when the Fermi level is located in the upper part of the band and vice versa. This behavior is similar to that of $\bar{N}_1{}^\sigma$ as a function of $\bar{v}_1{}^\sigma$. We may thus expect from (5·7a) that the second term $E^{(2)}$ behaves similarly to the third term $E^{(3)}$ except for the possible difference in sign. The quantity $\bar{v}_1{}^\sigma \bar{f}^\sigma_{2(1)}$ for the simple cubic lattice is plotted against $\bar{v}_1{}^\sigma$ in Fig. 9. These curves, aside from the relative shift along the ordinate, closely resemble the $\bar{N}_1{}^\sigma$ curves given in Fig. 2. Therefore, the ratio of the second term to the third term of (5·7) is approximately given by

$$E^{(2)}/E^{(3)} \simeq 2t/t^2 = 2/t\ .$$

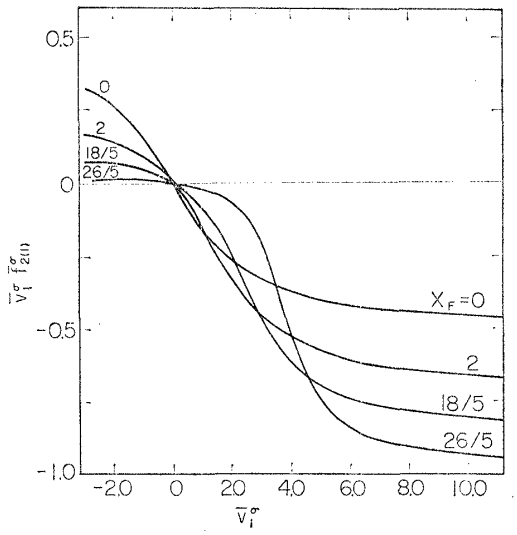

Fig. 9. Plot of $\bar{v}_1{}^\sigma \bar{f}^\sigma{}_{(1)}$ as a function of $\bar{v}_1{}^\sigma$ calculated by Eq. (5·8).

Here the sign of t is of particular importance. When t is positive, i.e. the net transfer integral between the neighboring impurity atoms is larger than the corresponding one in the host metal, the contributions of the second and third terms $E^{(2)}$ and $E^{(3)}$ add to enhance the contribution of the first term $E^{(1)}$. On the other hand, if t is negative, i.e. the transfer integral between neighboring impurity atoms is smaller than the corresponding one in the host metal, the contribution of the second term tends to reduce the first contribution $E^{(1)}$ although the third contribution $E^{(3)}$, which is opposite in sign to $E^{(2)}$, makes this tendency weak.

It is noticeable that when $t\simeq -1$, i.e. the total transfer integral between the impurity atoms almost vanishes, all the three contributions tend to cancel out resulting in a very weak coupling between the two moments. This conclusion is not so trivial as one might expect intuitively.

Finally the principal conclusions of this subsection are summarized as follows:
(1) The short range coupling between the two moments is mainly of local character, i.e. its sign is primarily determined by the occupation number of electrons in the impurity atoms and is less sensitive to the details of the band structure or the Fermi surface.
(2) Except for a certain range of negative values for t in which the transfer integral between the impurity atoms becomes very small and is of sign opposite

Downloaded from https://academic.oup.com/ptp/article/38/1/41/1900397 by guest on 21 August 2022

to that in the host metal, the following qualitative rule holds fairly generally: the impurity moments with nearly half-filled orbitals tend to couple with each other antiferromagnetically while those with larger number of electrons have increasing tendency towards ferromagnetic coupling.

§ 6. Change in moment due to interaction

Assuming that the effect of coupling between two impurity moments is small, we expand N_1^σ in powers of ΔN_i^σ as defined by (5·6). In lowest order in ΔN_i^σ, we obtain the following self-consistency equations for ΔN_1^σ:

$$\Delta N_1^\sigma + U_1 \bar{d}_1^\sigma \Delta N_1^{-\sigma} = \bar{C}_{12}^\sigma \tag{6·1}$$

with

$$\bar{d}_1^\sigma = \pi^{-1} \operatorname{Im} \int^{\epsilon_F} d\epsilon [g_{11}(\epsilon)]^2 [1 - \bar{V}_1^\sigma g_{11}(\epsilon)]^{-2}$$

and

$$\begin{aligned} \bar{C}_{12}^\sigma = -\pi^{-1} \operatorname{Im} \int^{\epsilon_F} d\epsilon & [1 - \bar{V}_1^\sigma g_{11}(\epsilon)]^{-2} [1 - \bar{V}_2^\sigma g_{11}(\epsilon)]^{-1} \\ & \times \{ \bar{V}_2^\sigma g_{12}(\epsilon) g_{21}(\epsilon) + T_{12} [g_{12}(\epsilon) + g_{21}(\epsilon)] g_{11}(\epsilon) \\ & + T_{12}^2 [g_{11}(\epsilon)]^3 \}. \end{aligned} \tag{6·2}$$

Solutions for Eq. (6·1) are

$$\Delta N_1^\sigma = (1 - U_1^2 \bar{d}_1^\uparrow \bar{d}_1^\downarrow)^{-1} (\bar{C}_{12}^\sigma - U_1 \bar{d}_1^\sigma \bar{C}_{12}^{-\sigma}). \tag{6·3}$$

The changes in number of electrons and in the moment of the first impurity atom are given by

$$\left.\begin{matrix} \Delta N_1 \\ \Delta M_1 \end{matrix}\right\} = (\Delta N_1^\uparrow \pm \Delta N_1^\downarrow)/2 = (1 - U_1^2 \bar{d}_1^\uparrow \bar{d}_1^\downarrow)^{-1} \left\{\begin{matrix} (1 - U_1 \bar{d}_1) \bar{C}_{12} + U_1 \bar{d}_1' \bar{C}_{12}' \\ (1 + U_1 \bar{d}_1) \bar{C}_{12}' - U_1 \bar{d}_1' \bar{C}_{12} \end{matrix}\right.$$

with

$$\left.\begin{matrix} \bar{C}_{12} \\ \bar{C}_{12}' \end{matrix}\right\} = (\bar{C}_{12}^\uparrow \pm \bar{C}_{12}^\downarrow)/2, \qquad \left.\begin{matrix} \bar{d}_1 \\ \bar{d}_1' \end{matrix}\right\} = (\bar{d}_1^\uparrow \pm \bar{d}_1^\downarrow)/2. \tag{6·4}$$

In the case where the first impurity atom is non-magnetic by itself, we can put $\bar{d}_1' = 0$ in Eq. (6·4), so that the induced polarization of an originally non-magnetic impurity atom is given by

$$\Delta M_1 = (1 - U_1 \bar{d}_1)^{-1} \bar{C}_{12}'. \tag{6·5}$$

Since we have $1 - U_1 \bar{d}_1 > 0$ in this case, the sign of the spin polarization is determined by the sign of $\bar{C}_{12}$.

Downloaded from https://academic.oup.com/ptp/article/38/1/41/1900397 by guest on 21 August 2022

As is easily seen, $(\bar{d}_1^{\uparrow}+\bar{d}_1^{\downarrow})/2$ represents the differential local susceptibility*) for the first impurity atom and $(d_1^{\uparrow}-d_1^{\downarrow})/2$, the accompanying change in the number of electrons in the same atom. At the critical boundary for the appearance of the localized moment, we have $\bar{d}_1^{\uparrow}=\bar{d}_1^{\downarrow}=U_1^{-1}$. Thus from (6·4) we see that the change in moment of an impurity atom due to the coupling with another impurity atom can be quite large when the impurity concerned is near the critical boundary for magnetization. Except near the critical boundary the order of magnitude of this change is given by $\bar{C}_{12}^{\sigma}$. Discussion thus goes quite parallel to the case of the Anderson model.[6] We shall present here some of the results of numerical calculation of $\bar{C}_{12}^{\sigma}$ for the simple cubic lattice model. We rewrite Eq. (6·2) as

$$\bar{C}_{12}^{\sigma}=\bar{C}_{12}^{\sigma(1)}+2t\bar{C}_{12}^{\sigma(2)}+t^2\bar{C}_{12}^{\sigma(3)}. \quad (6\cdot6)$$

Numerical values for $\bar{C}_{12}^{\sigma(i)}$ are plotted in Fig. 10a, b, and c, against $\bar{N}_1^{\sigma}$ for various values of $\bar{N}_2^{\sigma}$, the Fermi level being taken in the middle of the band. Even for the different values of the Fermi level the results are qualitatively similar to those shown in Fig. 10.

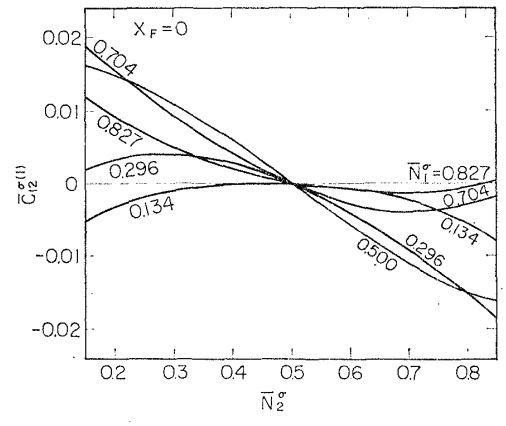

(a)

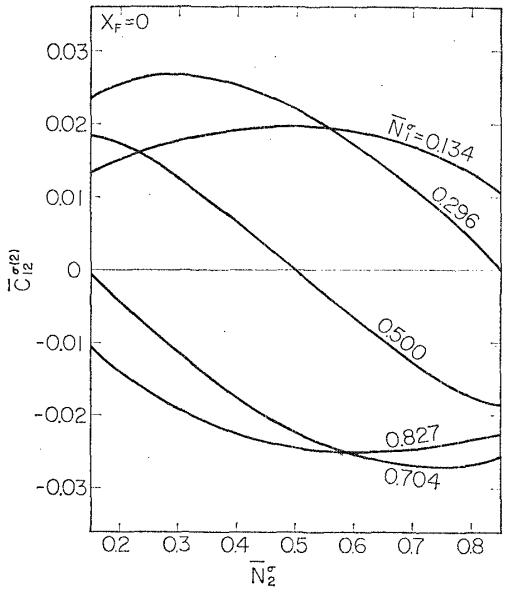

(b)

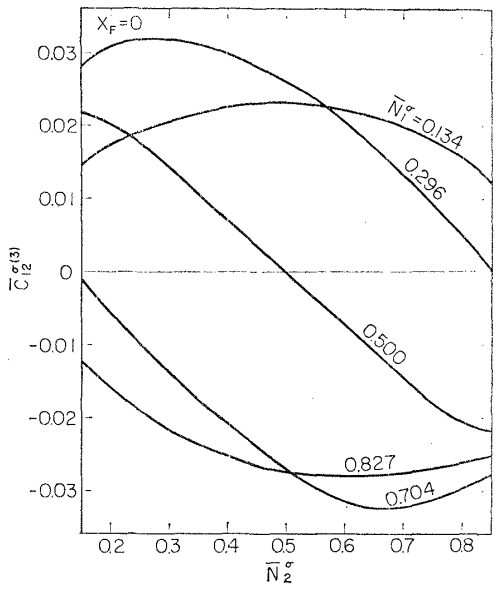

(c)

Fig. 10. Calculated curves for (*a*) $\bar{C}_{12}{}^{\sigma(1)}$, (b) $\bar{C}_{12}{}^{\sigma(2)}$ and (c) $\bar{C}_{12}{}^{\sigma(3)}$ versus $\bar{N}_2{}^{\sigma}$ for various values of $\bar{N}_1{}^{\sigma}$ with $x_F=0$.

*) The induced moment in Bohr magnetons of the impurity atom due to a unit magnetic field applied locally on this atom.

Downloaded from https://academic.oup.com/ptp/article/38/1/41/1900397 by guest on 21 August 2022

From the above formulas and the numerical values we can discuss the sign and the magnitude of the change in localized moments due to the interaction between two impurity atoms. The results are, as expected, qualitatively the same as in the case of the Anderson model[4] and so we shall not repeat them here.

§ 7. Critical boundary for the appearance of the moments

The critical boundary for the appearance of the impurity moment is affected by the presence of the second impurity atom. Let us discuss this problem by using non-local susceptibility of the alloy. We shall first assume that the non-magnetic self-consistent solution has been obtained for a metal with two impurity atoms 1 and 2. When the local external magnetic field, $\mathcal{H}_1$ at the first and $\mathcal{H}_2$ at the second impurity sites, is applied, the induced moments are described in terms of non-locals usceptibilities as follows:

$$\begin{aligned} M_1 &= F(1,1)\,(2\mu_B\mathcal{H}_1 + U_1 M_1) + F(1,2)\,(2\mu_B\mathcal{H}_2 + U_2 M_2), \\ M_2 &= F(2,1)\,(2\mu_B\mathcal{H}_1 + U_1 M_1) + F(2,2)\,(2\mu_B\mathcal{H}_2 + U_2 M_2), \end{aligned} \tag{7·1}$$

where $F(j,l)$ is $(2\mu_B)^{-2}$ times the non-local susceptibility for the alloy;

$$F(j,l) = (2\mu_B)^{-2}\chi(j,l) = \pi^{-1}\,\mathrm{Im}\int^{\epsilon_F} d\epsilon G_{jl}(\epsilon)\,G_{lj}(\epsilon). \tag{7·2}$$

The critical boundary is obtained from the condition that the homogeneous equation of (7·1) has a non-zero solution, i.e.

$$1-[U_1F(1,1)+U_2F(2,2)]+U_1U_2\{F(1,1)F(2,2)-[F(1,2)]^2\}=0, \tag{7·3}$$

where we have

$$M_1/M_2 = U_2F(1,2)/[1-U_1F(1,1)] = [1-U_2F(2,2)]/U_1F(2,1). \tag{7·4}$$

For brevity let us consider the following two cases:

(i) $U_1=U_2=U$.

The condition for the appearance of the moment is given by

$$U \geqslant U_c = [F(1,1) \pm F(1,2)]^{-1} \quad \text{for} \quad M_1/M_2 = \pm 1. \tag{7·5}$$

The upper and lower signs are taken for the parallel and antiparallel arrangements of two impurity moments, respectively.

(ii) $U_2=0$, $U_1\neq 0$.

We have

$$U_c = [F(1,1)]^{-1}$$

and

$$M_2/M_1 = U_1F(2,1). \tag{7·6}$$

Downloaded from https://academic.oup.com/ptp/article/38/1/41/1900397 by guest on 21 August 2022

As an example let us apply case (ii) to the problem of possible discontinuous occurence of the localized moment which has recently been proposed by Jaccarino et al. on experimental grounds.[9] In Fig. 11 we plot U_C given by Eq. (7·6) as a function of the number of electrons N_1 in the first impurity atom. The Fermi level is taken in the middle of the band. The dashed curve represents U_C for a single impurity, i.e. for $v_2=0$. The full curves give U_C in the presence of the second non-magnetic impurity with $v_2=0.6$, on the adjacent site; the upper and lower curves represent the results for the values of covalency parameters $t=1/4$ and $-1/2$, respectively. For $t=0$ the calculated curve of U_C in the presence of the second impurity on either the nearest or the second neighboring site of the impurity concerned, falls very close to the dashed curve. When the value of U_1 lies in the region between the dashed and the solid upper lines in this figure, we can certainly see the discontinuos occurrence of the impurity moment; the first impurity atom does not have a moment in the absence of the second impurity, while it does when the second impurity atom comes in the nearest neighboring site.

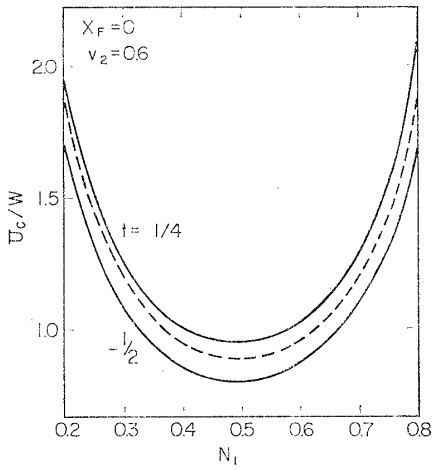

Fig. 11. Plot of the critical boundary for magnetization against N_1: dashed curve refers to the single impurity atom, and, upper and lower full curves refer respectively to the impurity for $t=1/4$ and $-1/2$ in the presence of the second impurity atom with $v_2=0.6$.

Although the above model is an extremely simple one, it may qualitatively represent the situation for the body-centered cubic Nb-Mo alloys with Fe impurity, discussed by Jaccarino et al.,[9] i.e. Fe impurity atom in these alloys is discontinuosly demagnetized when at least one of the nearest neighboring sites is occupied by Nb atom. Another example is the case of Co impurity in Rh-Pd alloys. A Co impurity atom is discontinuosly magnetized if at leasst one Pd atom lies next to it.[9] Although we have made no calculation corresponding to this situation, results are expected to be promising, considering the results of the previous theory based on the Anderson model.[4]

§ 8. Conclusions

We have examined the effects of the interaction between localized moments in metals using the Wolff-Clogston tight-binding model. The results for a pair of neighboring atoms are essentially equivatent to those derived earlier on the Anderson model.[4] It is particularly significant and gratifying that the effect of short range interaction is shown to be primarily of local origin, and independent of the initial model, thus describable in terms of the number of electrons per im-

Downloaded from https://academic.oup.com/ptp/article/38/1/41/1900397 by guest on 21 August 2022

purity atom and the strength of the local bond. As mentioned in the earlier articles,[4),7)] the general rule for the sign of the spin polarization and the spin coupling deduced on this point of view, explains successfully numbers of experimental data. Although the real state of transition metals and alloys may be far more complicated than what these models describe, we believe that the above conclusion would have general qualitative validity and relevance to the future better theory of magnetism of these metals and alloys.

For a distant pair of impurity atoms, the expression obtained for the effective exchange energy is rather simple including only the phase shifts and the information on the band structure only near the Fermi surface. The phase shifts may be estimated approximately from the electron occupation number and the moments of the impurity atoms by using the Friedel sum rule. For qualitative estimation of the coupling constants, there appears no parameter which is difficult to estimate, like the *s-d* exchange or *s-d* admixture matrix elements. This interaction, as extended to the five-fold *d*-band, is considered to play a predominant role in the magnetic properties of dilute magnetic alloys of transition metals, for example Fe-4*d* alloys.

Acknowledgements

We would like to thank Dr. K. Inoue and Dr. H. Takahashi of the computing center of ISSP for helpful advice.

References

1) J. Friedel, Nuovo Cim. **7** (1958), 287; *Metallic Solid Solutions*, xix-1, edited by J. Friedel and A. Guinier (W. A. Benjamin, Inc., 1963).
2) P. W. Anderson, Phys. Rev. **124** (1961), 41.
3) P. A. Wolff, Phys. Rev. **124** (1961), 1030; A. M. Clogston, Phys. Rev. **125** (1962), 439.
4) For references see the following review article: T. Moriya, *Proceedings of the International School of Physics "Enrico Fermi"* (1966), to be published.
5) S. Alexander and P. W. Anderson, Phys. Rev. **133** (1964), A 1594.
6) T. Moriya, Prog. Theor. Phys. **33** (1965), 157.
7) D. J. Kim and Y. Nagaoka, Prog. Theor. Phys. **30** (1963), 743.
B. Caroli, A. Blandin and J. Friedel, to be published.
8) B. Caroli, to be published.
9) V. Jaccarino, L. R. Walker and G. K. Wertheim, Phys. Rev. Letters **13** (1964), 752.
10) T. Moriya, Prog. Theor. Phys. **34** (1965), 329.
11) G. F. Koster, Phys, Rev. **95** (1954), 1436,
12) A. Blandin, J. phys. radium **22** (1961), 507.
13) G. F. Koster and J. C. Slater, Phys. Rev. **96** (1954), 1208.

Downloaded from https://academic.oup.com/ptp/article/38/1/41/1900397 by guest on 21 August 2022